Probabilistic streamflow forecasts for Mississippi River navigation risk and parametric insurance

Short title: Mississippi River forecasts and navigation risk

Jennifer Nakamura[1,*], Xander Nakamura[2], Upmanu Lall[3,4]

[1] Lamont-Doherty Earth Observatory of Columbia University, Ocean and Climate Physics, Palisades, New York, 10964, USA.

[2] Park Ridge High School, Park Ridge, New Jersey, 07656, USA.

[3] Arizona State University, School of Complex Adaptive Systems, Tempe, Arizona, 85287, USA.

[4] Columbia University, Earth and Environmental Engineering, New York, New York, 10027, USA.

* Correspondence: jennie@ldeo.columbia.edu (J.N.)

This manuscript is a non-peer reviewed preprint submitted to EarthArXiv. This version has been submitted to PLOS Water.

Abstract

Mississippi River navigation is disrupted by both low and high water extremes, yet shippers, ports, and terminals lack a simple instrument to transfer that risk. We test whether probabilistic forecasts of monthly streamflow can provide useful navigation-risk information. Using pretrained Chronos-2 at three major Mississippi River subbasin outlets, we compute navigation risk probabilities, parametric insurance premiums, and basis risk using land surface, atmospheric, and ocean predictors. Land surface and moisture-budget predictors provide the strongest forecast, with a probabilistic forecast skill relative to climatology declining from 0.30 at one month to 0.08 at four months. A perfect-future experiment that supplies the observed future land state while withholding discharge retains much greater skill, 0.44 at one month and 0.34 at four months, showing that uncertainty in the future land conditions is the main source of loss of streamflow predictability. Low-, high-, and combined-water probabilities are evaluated at 1-4 months, to assess whether forecast-based risk pricing can send price signals for anticipatory action. Results support a 1-4 month decision time line and motivate initiating seasonal forecasts coupled to a land-surface or hydrologic model.

Keywords: Mississippi River; hydrologic extremes; probabilistic streamflow forecasting; navigation risk; parametric insurance; basis risk

1. Introduction

The Mississippi River system is an important corridor for affordable inland freight in the U.S., carrying a large share of the nation's grain exports, bulk agricultural inputs, and petroleum products at approximately a 10^{th} of rail and a 16^{th} of truck costs [1–3]. Navigability on this system is governed not by average conditions but by extremes: when river stage or flow falls below or above Coast Guard low-water and high-water thresholds, allowable vessel drafts are

restricted, tow sizes are reduced, and reaches may eventually be closed, due to low water or dangerous swift currents and submerged infrastructure [4–9]. The low-water droughts of 2022 and 2023, along with recurrent high-water events, show that these interruptions are frequent, costly, and increasingly variable [10]. Shippers, terminal operators, and downstream buyers currently bear the financial consequences of low- and high-water navigation disruptions directly, including reduced cargo volumes, shipment delays, higher transportation costs, and higher prices for goods, because no standardized, rapidly settling instrument exists to transfer this inland-navigation interruption risk.

In fall 2023, low water on the Mississippi forced grain shippers to load 500 to 700 fewer tons per barge, increasing the number of trips and the cost of moving the same amount of grain [11]. A parametric policy could help offset these losses by increasing payouts as river levels fall and operating restrictions become more severe. Because payments would be triggered by observed river conditions rather than documented losses, funds could be delivered quickly to help cover the added costs of disrupted barge movements.

Growing interest in parametric insurance is already evident along the Mississippi. In late 2024, the Mississippi River Cities and Towns Initiative (MRCTI) announced a flood insurance pilot designed to provide faster payouts with a simpler claims process [12]. In 2025, the program advanced as MRCTI and Munich Re finalized a mock-up policy using USGS river gauge data to set area flood-depth triggers for payouts [13]. Cities including Baton Rouge, Grafton, and Gretna expressed interest in the implementation phase [14]. The National Association of Insurance Commissioners (NAIC) also featured the project in its fall 2025 Affordability and Availability Playbook as a potential national model for weather resilience [15]. MRCTI and Munich Re are continuing to develop the program, with a mid-Mississippi pilot anticipated in 2027 [16]. Swiss

Re markets FLOW, a parametric insurance product that covers business losses associated with high or low water levels on European rivers, with payouts tied to specified river gauges [17]. Marsh has also discussed river-level parametric coverage for transport disruption, including a potential Mississippi River application [18].

These products show the potential for transferring river-related losses, but pricing could also provide a signal for action before navigation is disrupted. Under a conventional stationary approach, the cost of insurance (premium) is based on the historical probability of a payout and reflects average risk rather than conditions expected during a particular coverage period. Forecast-based pricing instead updates the premium as the predicted probability of a payout changes. If the premium remains fixed, buyers may wait to purchase coverage until forecasts indicate a greater chance of a payout. Khalil et al. [19] examined the predictability of an ENSO-based flood insurance index to identify when sales should close before the coming season's risk became clear.

Here we explore this forecast pricing approach for Mississippi River navigation. A higher forecast-based premium could signal a need to purchase coverage despite the higher cost, delay a shipment, arrange rail or truck transport, renegotiate shipment timing or transportation contracts, or store cargo until conditions improve. Storage, however, can add costs, and for grain shipments, it may increase spoilage risk in warm and/or humid conditions [20]. Forecast-based insurance pricing provides an application for the streamflow forecasts and a potential signal of changing navigation risk. We also examine how basis risk (risk that the payout does not match the actual loss) changes with the time between the forecast and the month being predicted.

Khalil et al. [19] also provide the statistical foundation for this analysis, linking an ENSO-based index to flood-threshold exceedance probabilities for Peru and using those probabilities to price a

parametric flood policy at an actuarially fair premium. They evaluated the stationarity and temporal clustering of the index exceedances used to determine payouts, as well as the basis risk introduced by using ENSO as a proxy. Employing this framework to inland navigation requires extending it to multiple river basins and navigation thresholds, incorporating probabilistic streamflow forecasts that estimate the probability of crossing each trigger, and evaluating the basis risk across different forecast leads.

Convolutional neural networks have been used for water-level forecasting [21] and streamflow projection [22]. Yang et al. combined a deep convolutional network with a Transformer for monthly hydroclimatic forecasting [23]. Spatial atmospheric patterns have also been used to forecast large-scale circulation regimes with deformable convolutional networks [24]. More generally, dilated convolutions can aggregate information across spatial scales without reducing resolution [25]. These applications motivate testing whether learned atmospheric representations add information beyond basin-average land conditions.

The forecast layer is where recent advances in machine learning are particularly useful. Pretrained time-series foundation models such as Chronos [26] and Chronos-2 [27] can generate probabilistic forecasts directly from a target history and optional covariates without task specific retraining. This provides a convenient way to test whether physically motivated hydrologic, atmospheric, and oceanic predictors add information beyond the discharge history itself. For forecast-based pricing to help shippers, forecasts must be reliable and give them enough time to change their plans.

Forecast lead and calendar season are treated separately by issuing a forecast from every monthly origin. The same calendar month can be evaluated at different leads, and the same lead can be

evaluated in every season. The primary operational horizon emphasized here is 1-4 months. Leads 1-12 are retained to show the full decay of skill.

This study makes several contributions. We develop a leakage-controlled monthly rolling-origin pipeline for probabilistic discharge forecasting and quantify both the 1-4 month operational horizon that showed skill, and the complete 1-12 month skill decay as the main contribution. We compare land-surface, learned atmospheric, and ocean predictor pathways and use an independent staged regression plus a perfect-future land-surface diagnostic to identify the source of additional predictability. Finally, as a general motivation, we map the forecast distributions to low-water, high-water, and combined navigation risk, low-water return-period pricing, basis risk, and record-stationarity diagnostics.

2. Data and Study Area

2.1. Streamflow observations

Three sub-basins were selected for this study: the Upper Mississippi at Grafton, Illinois (USGS 05587450); the Missouri at Hermann, Missouri (USGS 06934500); and the Lower Mississippi outflow at Tarbert Landing (USACE 01100Q). Each has a long, continuous, and highly complete daily discharge record at the subbasin outlet. The USGS gauges provide more than 90 years of data with greater than 98 percent daily coverage, supplying the observational basis required for forecast development and validation. Also, the three gauges span distinct hydroclimatic regimes. The Upper Mississippi at Grafton is an upper-basin system that has a combination of snowmelt and rainfall. The Missouri at Hermann is a semi-arid plains river substantially influenced by upstream reservoir regulation. Tarbert Landing represents the combined-system outflow near the Old River Control Structure. Together, these sites allow the forecasting and pricing framework to be evaluated across several flow behaviors rather than along a single river reach (Fig 1).

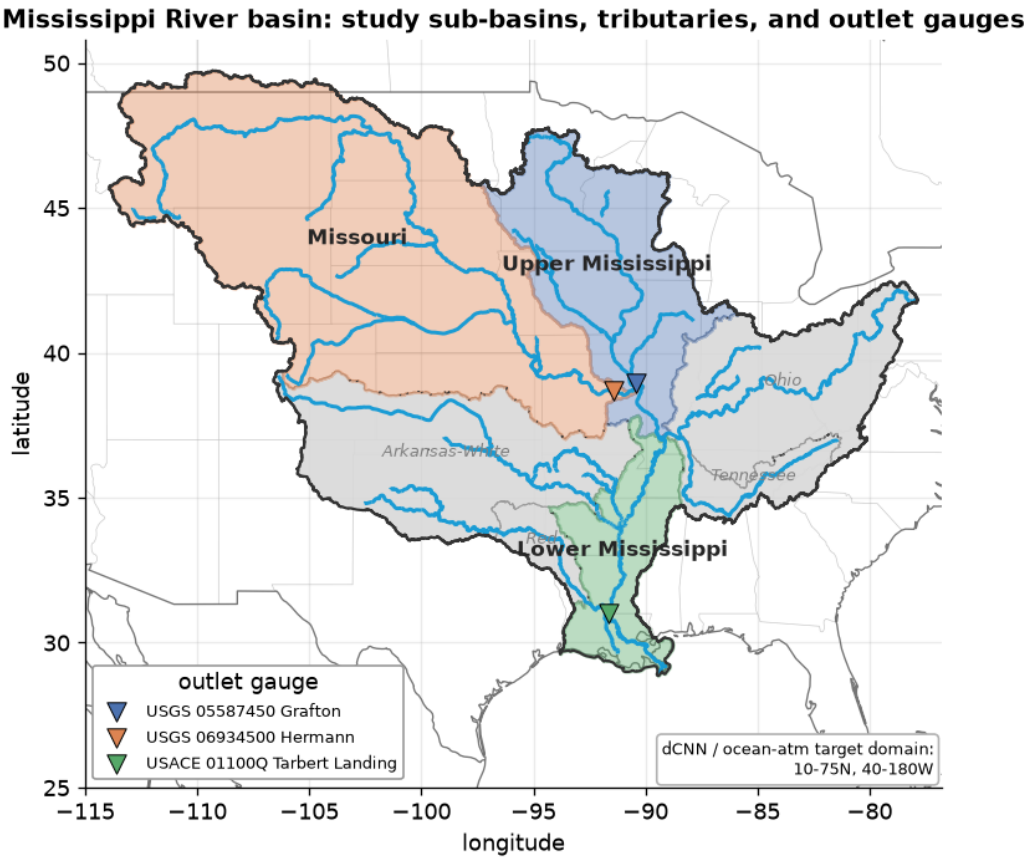


Fig 1. Study subbasins and outlet gauges: drainage-basins for the Mississippi River basin, with the three forecast gauges marked.

Daily discharge is aggregated to monthly means. The annual minimum monthly discharge for each basin is then kept for the return-period analysis. Primary pricing and stationarity analyses use the common 1979-2024 evaluation period. The complete gauge records are analyzed separately as long-record sensitivity tests. For the Upper Mississippi and Missouri, the candidate stage records are from the same USGS sites used for discharge at Grafton and Hermann (Table 1). For the Lower Mississippi, the candidate stage record is from Red River Landing (gauge 01120), the nearest suitable Lower Mississippi gauge below the Old River Control Structure (Table 1). No usable stage-discharge rating was obtained in the analysis, so the reported high-water thresholds and probabilities use discharge proxies rather than these stage records.

Table 1. Study basins, forecast gauges, and hydroclimatic regimes.

Basin (forecast gauge)	Station ID	Regime	Stage source
Upper Mississippi (Grafton, IL)	USGS 05587450	Snowmelt + rainfall, pooled reach	Same as flow gauge
Missouri (Hermann, MO)	USGS 06934500	Semi-arid plains, reservoir-regulated	Same as flow gauge
Lower Mississippi (Tarbert Landing)	USACE 01100Q	Combined-system outflow	Red River Landing (01120)

An extension to additional subbasins on the Ohio, Tennessee, Arkansas, and Red rivers was also evaluated, but these basins were not included because suitable continuous subbasin outlet discharge records were unavailable. Candidate gauges we looked at had been discontinued, or operated primarily as water-quality stations, or had large gaps from shutting down for major navigation-system construction. The additional reaches are reserved for future work incorporating USACE stage-based flow records with rating curves [28].

2.2. Predictor variables and their spatial representation

Predictors are grouped according to how their physical role is best represented spatially. Three predictor pathways are provided to the forecasting model.

Monthly European Centre for Medium-Range Weather Forecasts fifth-generation atmospheric reanalysis (ERA5) [29] land-surface variables include evaporation, precipitation, 2 m temperature, soil moisture, and snow. Each variable is reduced to an area weighted basin mean because basin-average conditions are most directly related to catchment discharge. Vertically integrated moisture-budget terms, including moisture-flux divergence and its mean-flow components, are calculated following Seager and Henderson [30] and reduced in the same way. Slowly varying ocean conditions are represented by sea-surface-temperature anomalies (SST) and 0-300 m total ocean-heat-content anomalies. Met Office Hadley Centre Sea Ice and Sea

Surface Temperature dataset (HadISST) [31] provides Niño-region SST indices, the Pacific Decadal Oscillation (PDO), the Atlantic Multidecadal Oscillation (AMO), and lagged Niño-3.4 indices. These ocean predictors are separate from the LAND land-surface covariates and reach the forecasting model through two alternative arms. The precursor arm uses global HadISST SST and Ocean ReAnalysis System 5 (ORAS5) [32] 0-300 m ocean heat content anomalies as gridded fields. The ocean-direct arm instead reduces that same 0-300 m heat-content field to a few interpretable proxies, each computed as an area weighted box mean of the heat-content anomaly: an equatorial-Pacific warm-water-volume proxy (5°S to 5°N, 120°E to 80°W); a zonal-tilt proxy taken as a western box (5°S to 5°N, 120°E to 155°W) minus an eastern box (5°S to 5°N, 155°W to 80°W); and broad Indo-Pacific (20°S to 20°N, 40°E to 80°W) and Atlantic (0° to 60°N, 80°W to 0°) heat-content means. Each proxy enters at explicit monthly lags, giving the model the ocean state a fixed number of months before the target month. Upper-air circulation variables are retained as two-dimensional anomaly fields rather than reduced to basin averages. These variables include geopotential height, zonal and meridional winds, and mean sea-level pressure over 10-75 °N, 180-40 °W. Their potential predictive value lies in the spatial pattern of atmospheric circulation, which would be lost through basin averaging. For example, opposing wind anomalies could average to nearly zero across a region even when they form a strong circulation pattern. A deep convolutional neural network converts these fields into a compact monthly representation. This representation is then combined with the basin mean and ocean covariates to form the full predictor vector.

2.3. Navigation thresholds from Waterways Action Plans

Navigation-disruption thresholds are drawn from the Waterways Action Plan (WAP) annexes, which provide multiple location-specific stage thresholds. Because the forecast analysis is

conducted in discharge, a WAP threshold is used directly only when it is available in discharge units at the forecast gauge. This applies to the Missouri at Hermann, where the annex provides a 47,000 cfs low-water Action threshold [8]. For the Upper Mississippi at Grafton and the Lower Mississippi at Tarbert Landing, the WAP low-water stage thresholds were not converted to discharge in the present analysis, so historical 10th-percentile discharge values are used as explicitly identified proxies. High-water WAP stage thresholds were likewise not converted to discharge, so historical 90th-percentile discharge proxies are used for all three basins. Accordingly, the high-water and combined low-or-high results, as well as the proxy-based low-water results for Grafton and Tarbert Landing, are interpreted as navigation-risk diagnostics rather than fully operational WAP-based contracts.

3. Methods

3.1. Feature construction and leakage control (Step 1-2)

The monthly predictor dataset is constructed to prevent future information from entering the forecasting process. ERA5 surface fields and the moisture-budget terms are area-averaged to per-basin monthly series; discharge targets for the three gauges are read into a single monthly frame; ocean predictors are computed from HadISST and ORAS5; and the WAP threshold was recorded. All predictors except the gridded upper-air and ocean fields are combined into a single covariate dataset. The upper-air fields retain their two-dimensional spatial structure and are passed separately to the convolutional encoder. Calendar-month climatologies, the upper-air encoder, the ocean-to-atmosphere encoder, and the North Pacific empirical orthogonal function (EOF) used to make the PDO index are estimated from the initial 1959-1978 pre-evaluation period and then frozen. Code step 1-2 defines the initial training and evaluation boundaries. Code step 3 then advances the forecast origin one month at a time from December 1978 through

November 2024, using only data available through each origin. Forecasts extend up to 12 months, subject to the evaluation period's end. Lead-to-lead skill comparisons use the common December 1979-December 2024 verification window, so all 12 leads are evaluated against the same target months.

3.2. Probabilistic streamflow forecasting with a foundation model and ridge regression check (Step 3)

Chronos-2 forecasts monthly discharge directly from the pretrained model with no task-specific training. For each monthly rolling origin, the model receives discharge history and selected covariates only through the origin month. Observed covariates from the forecast period are not supplied to the operational forecast. Each origin produces up to a 12-month horizon. Forecast distributions are generated on quantiles 0.01-0.99 so that both low- and high-flow tails are resolved. Chronos-2 forecasts discharge in its original units. Forecast skill is compared using the same start dates and target months for every model. LAND uses basin land-surface and moisture-budget variables. ATM adds upper-air atmospheric information, OCEAN adds ocean-atmosphere precursor signals and their lags, and HCP adds ocean heat-content indices. FULL combines the predictor blocks. Base Chronos-2 uses discharge history alone. Climatology is computed from historical training data only. Forecasts are evaluated using the Continuous Ranked Probability Score (CRPS), which compares the forecast probability distribution with observed discharge. We approximate CRPS from the mean quantile loss across the 0.01-0.99 forecast quantiles. Forecast skill is then measured relative to historical climatology, with positive values indicating better performance than climatology. For comparing configurations, performance is averaged across the 1-12 month verification window, while each forecast lead is also scored separately. Calendar-month skill is calculated independently at leads 1-4.

10-90% interval coverage and the frequency of low- and high-flow forecasts are evaluated for leads 1-4. CRPS is calculated separately for recorded low-water and high-water tails over those leads. A perfect-future LAND diagnostic supplies the observed future LAND covariates for each forecast horizon while still withholding future discharge. This is a potential-skill benchmark, not an operational forecast. It is carried through diagnostic risk, pricing, and basis-risk calculations to quantify how much improvement could result from forecasting the future land state.

As an independent check of whether the additional predictor groups contain information beyond LAND, we use a staged ridge-regression diagnostic. Within each out-of-sample annual-origin fold, a ridge regression is first fit to standardized log-transformed discharge using the LAND predictors. A second ridge regression is then fit to the residuals from the LAND model using one additional predictor block at a time. Predictors are standardized within the training data, and the ridge penalty is selected by cross-validation. Incremental out-of-sample R^2 measures whether adding each block improves prediction relative to LAND alone; negative values indicate no additional predictive information.

3.3. From forecast to disruption probability (Step 4)

Navigation risk is computed directly from each predictive distribution. Low- and high-water probabilities are the forecast probabilities of discharge falling below or exceeding the respective basin thresholds. The combined probability is the sum of these two non-overlapping risks, limited to a maximum of one. These probabilities are evaluated over the same verification period at 1- to 4- month lead times and compared with observed low-water, high-water, and two-sided event rates. The main multi-lead analysis uses the forecast probabilities directly so that all lead times are evaluated consistently.

3.4. Parametric-insurance design and pricing (Step 5)

Low-water insurance triggers are set at 10-, 20-, and 50-year return levels using annual minimum monthly discharge from 1979-2024. Observed thresholds are used when the record is long enough to support them. Because the 50-year level lies beyond the 45-46 year primary records, the 50-year trigger is treated as a sensitivity case. A Gumbel estimate is used when it yields a positive threshold; where the fitted Gumbel estimate is negative, as for the Missouri, the 2nd percentile of annual minimum discharge is used instead and flagged as a fallback. For each lead from 1-4 months, the actuarially fair premium per $1 maximum payout is the expected payout based only on the forecast risk, without administrative costs or profit. For the binary low-water return-period policies used here, this equals the forecast probability that discharge breaches the low-water trigger. The same fair-premium interpretation is applied to the low-water, high-water, and combined navigation-threshold products, with high-water and combined values treated as diagnostic because the high-water thresholds are proxy-based. The perfect-future LAND version is calculated only as a diagnostic comparison.

Robustness of the low-water pricing results is assessed with a five-year payout-count (0 to 5) bootstrap. Annual breach indicators are resampled 2,000 times using two methods: independent resampling of individual years and resampling of contiguous three-year blocks, and the ratio of block-bootstrap to independent-year payout-count variance is used to assess temporal clustering. A buyer-focused sensitivity combines the 10-, 20-, and 50-year policies to approximate an assumed loss pattern in which losses increase as river flow falls. For this sensitivity analysis, the assumed loss is zero at or above the 10-year low-flow threshold, increases linearly to 1 at the 20-year threshold, and continues increasing to a maximum of 2 at more severe low flows. This is the loss function used in the policy-combination calculation rather than being estimated from

observed financial losses. Basis risk is evaluated across leads 1-4 for low-water, high-water, and combined low-or-high navigation risk. For each navigation risk type, a single forecast-probability threshold for triggering a payout is selected to balance missed disruptions and unnecessary payouts. The threshold minimizes the average of these two error rates across all three basins and leads 1-4. The same threshold is then applied to the perfect-future LAND diagnostic. Mann-Kendall and Pettitt tests are applied to the 1979-2024 annual-minimum series used for low-water pricing, with complete gauge records retained as a sensitivity analysis.

4. Results

4.1. Forecast skill, lead dependence, and covariate comparison

LAND (Fig 2a) provides the strongest operational forecast performance and retains useful skill through 1-4 months (Fig 2b). Mean CRPS skill versus climatology is 0.301 at lead 1, 0.153 at lead 2, 0.101 at lead 3, and 0.078 at lead 4 (Fig 2b). Skill remains slightly positive through lead 11. Thus, 1-4 months is emphasized as the principal operational horizon, while the full 1-12-month curve shows that longer-lead skill gradually drops (Fig 2b).

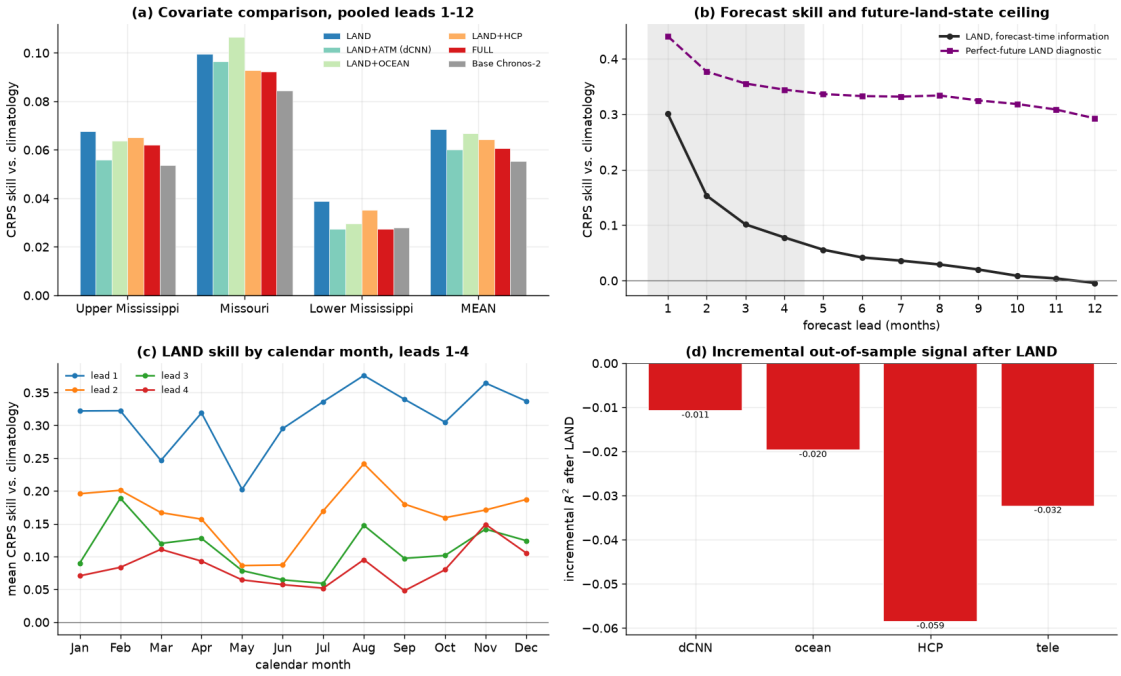


Fig 2. Forecast performance and the contribution of the different covariates. (a) CRPS skill relative to climatology for the six forecast configurations, evaluated across leads 1-12 over the common verification period. (b) LAND skill by forecast lead alongside the perfect-future LAND diagnostic, with shading indicating 1-4 months. (c) Mean LAND skill by calendar month at fixed leads 1-4. (d) Incremental out-of-sample R2 from adding each predictor block after LAND in the independent staged ridge diagnostic. dCNN denotes the deep convolutional neural-network representation of upper-air circulation; ocean is the learned ocean-to-atmosphere representation based on sea-surface temperature and 0-300 m ocean heat content; HCP comprises direct 0-300 m ocean heat-content precursor indices; and tele comprises scalar teleconnection indices, including Niño-3.4, AMO, IOD, PDO, and lagged Niño-3.4 measures.

LAND performs best overall, with land-surface information providing most of the forecast skill. Across leads 1-12, LAND has the highest mean CRPS skill (0.069), and adding other predictor types does not improve performance (Table 2; Fig 2a). At leads 1-4, skill remains positive on average across basins in every month, but declines with lead time (Fig 2c). Interestingly, the skill

peaks in August for leads 1 and 2 months, February for lead 3, and November for lead 4, so the timing of maximum predictability is lead dependent. The independent staged ridge regression supports the Chronos-2 comparison. LAND alone explains about 38% of out-of-sample variance in standardized log discharge, while every additional predictor block reduces out-of-sample performance: incremental R^2 is −0.011 for dCNN, −0.020 for the ocean block, −0.059 for HCP, and −0.032 for the teleconnection indices (Fig. 2d).

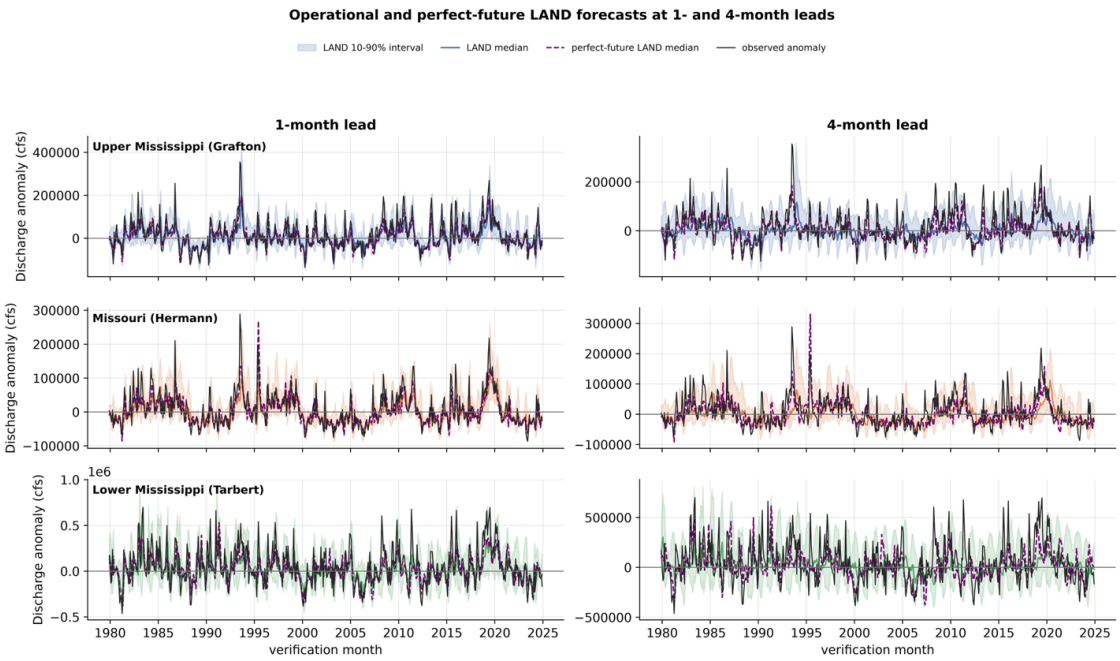
Table 2. CRPS skill versus climatology (>0 beats climatology) by basin and forecast configuration, calculated using all forecasts from leads 1-12 over the common verification period. LAND uses basin land-surface and moisture-budget variables; LAND + ATM (dCNN) adds a deep convolutional neural network representation of upper-air circulation; LAND + OCEAN adds the learned ocean-to-atmosphere precursor representation; LAND + HCP adds direct 0-300 m ocean heat-content precursor indices; FULL combines these predictor blocks; and Base Chronos-2 uses discharge history alone. LAND is the selected operational configuration.

Configuration	Upper Miss.	Missouri	Lower Miss.	Mean
LAND	0.068	0.099	0.039	0.069
LAND + ATM (dCNN)	0.056	0.097	0.027	0.060
LAND + OCEAN	0.064	0.107	0.030	0.067
LAND + HCP	0.065	0.093	0.035	0.064
FULL	0.062	0.092	0.027	0.061
Base Chronos-2	0.054	0.084	0.028	0.055

4.2. Predictive distributions and the perfect-future LAND gap

The perfect-future LAND diagnostic shows considerable predictability that is not available to the operational forecast. Mean CRPS skill is 0.441, 0.377, 0.355, and 0.344 at leads 1-4, compared with 0.301, 0.153, 0.101, and 0.078 for operational LAND (Fig 2b, dashed). The gap widens

rapidly with lead and remains large through the end of the forecast horizon: at lead 9, operational mean skill is 0.020 while perfect-future LAND is 0.325; at lead 12 the values are -0.004 and 0.293. The basin-level comparison shows the same result. At lead 4, perfect-future skill is 0.492 for the Upper Mississippi, 0.334 for the Missouri, and 0.207 for the Lower Mississippi, compared with operational values of 0.069, 0.129, and 0.035 (S1 Fig). Fig 3 shows that the perfect-future median retains much more of the observed anomaly structure at four months. The 10-90% forecast interval contains the observed streamflow close to the expected 80% of the time in the Upper Mississippi and Missouri, but less often in the Lower Mississippi, particularly beyond the one-month lead. Coverage below 0.80 indicates that the forecast range is too narrow or biased relative to the observed variability. Perfect-future LAND improves CRPS but does not consistently improve coverage (S2 Fig).



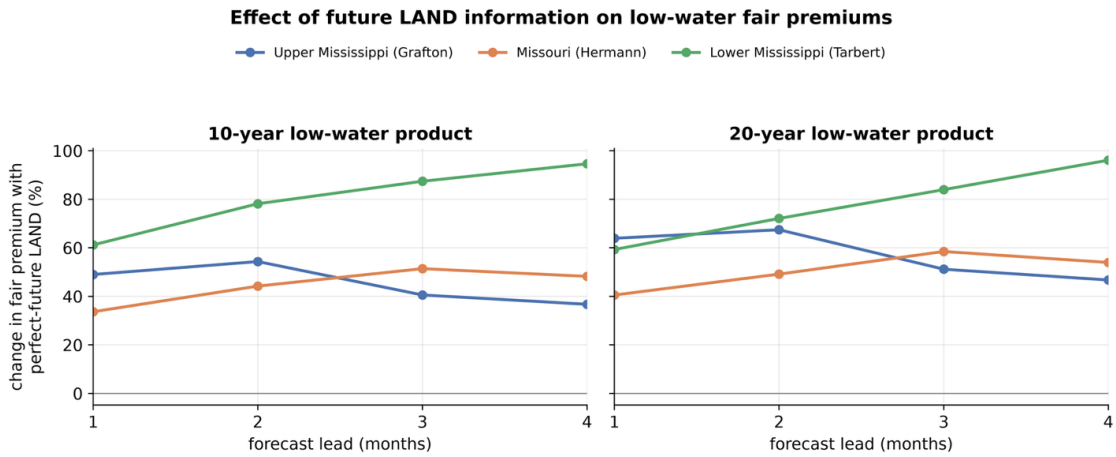
330

331 **Fig 3.** Operational LAND and perfect-future LAND discharge forecasts at 1- (left) and 4- (right)
332 month leads. For each basin, the operational LAND median (solid color) and 10-90% predictive
333 interval (shaded) are shown with the observed discharge anomaly (solid black), and the dashed
334 line shows the perfect-future LAND median. Anomalies are relative to the historical mean for
335 each rolling-origin forecast.

336 **4.3. Low-water return-period pricing across 1-4 months**

337 The perfect-future premiums are not intended as an operational pricing approach. They show
338 how much forecast-based pricing could change if future land conditions were predicted more
339 accurately, providing a motivation for improving the seasonal hydrologic forecast. Low-water
340 pricing is evaluated across 1-4 months. The 10- and 20-year triggers are supported by the
341 historical record in all three basins, so Fig 4 focuses on those products. In every case, perfect-
342 future LAND gives a higher fair premium than operational LAND. The difference is 0.0063-
343 0.0140 per $1 of maximum payout for the 10-year product and 0.0051-0.0107 for the 20-year
344 product. Although the amounts seem small, for a million dollar payment this translates to a

345 $6,300 to $14,000 for the 10-year and $5,100 to $10,700 for the 20-year difference in premium.
346 The largest difference occurs for the Upper Mississippi 10-year product at lead 2, where the fair
347 premium increases from 0.0258 to 0.0398. For the Lower Mississippi 10-year product, the
348 difference increases from 0.0063 at lead 1 to 0.0113 at lead 4, consistent with the widening
349 forecast-information gap with time. S1 Table provides all lead-specific values for the supported
350 products. The 50-year trigger lies outside the 45-46 year empirical support and is retained as a
351 sensitivity case in the return-period analysis rather than emphasized in the pricing comparison.



352
353 **Fig 4.** Effect of future LAND information on low-water fair premiums across leads 1-4. Change
354 in fair premium per $1 maximum payout between forecast and perfect-future for the 10- (left)
355 and 20-year (right) low-water products. Numerical values are given in S1 Table.

356 The block bootstrap shows modest and inconsistent temporal clustering for the data supported
357 10- and 20-year policies. For the 10- and 20-year triggers, respectively, clustering ratios are
358 1.129 and 1.240 for the Lower Mississippi, 1.269 and 0.899 for the Missouri, and 1.277 and
359 0.940 for the Upper Mississippi. Ratios above one indicate greater variability in the number of
360 payouts occurring over a five-year period when three-year blocks are preserved than when years
361 are resampled independently. Ratios below one indicate no increase in payout variability from
362 preserving that persistence. The 50-year case is too sparse for a stable clustering assessment: no

observed breach occurs in the Lower or Upper Mississippi primary record, and only one occurs in the Missouri record. Using the illustrative loss function defined in Methods, the fitted policy weights on the 10-, 20-, and 50-year policies were 0.559/1.186/0.000 for the Lower Mississippi, 0.624/0.625/0.751 for the Missouri, and 0.472/0.866/0.000 for the Upper Mississippi. Because this loss function is illustrative and the 50-year trigger is retained only as a sensitivity case, these weights illustrate how the policies can be combined rather than prescribe a contract design.

4.4. Low-water, high-water, and combined navigation risk

Predictive skill in both navigation-relevant tails degrades with lead, while perfect-future LAND substantially reduces CRPS for both low- and high-water months across leads 1-4 (Fig 5). The forecast distributions also yield low-water, high-water, and combined low-or-high event probabilities, with detailed basin- and lead-specific values given in S2 Table. The basin-specific navigation thresholds and observed event rates are summarized in Table 3. Across leads 1-4 during the December 1979-December 2024 verification period, the observed frequencies of low, high, and two sided events were 0.057/0.181/0.238 for the Lower Mississippi, 0.179/0.201/0.381 for the Missouri, and 0.030/0.212/0.242 for the Upper Mississippi. The average forecast probabilities for these events changed little from one to four month lead times. At lead 1 they are 0.038/0.165/0.202 for the Lower Mississippi, 0.180/0.186/0.366 for the Missouri, and 0.029/0.175/0.204 for the Upper Mississippi; by lead 4 they are 0.043/0.171/0.215, 0.173/0.185/0.357, and 0.035/0.175/0.210, respectively. The perfect-future probabilities are generally closer to the observed low-water rate in the Lower Mississippi and retain similar high-water frequencies across leads 1-4. However, agreement in mean event frequency does not show whether elevated probabilities occur in the months when navigation-threshold events actually occur. This timing is evaluated through the basis-risk analysis in Section 4.5.

Table 3. Low-water and high-water navigation thresholds and detected event rates on the balanced verification window. Low-water is based on the WAP Action discharge threshold for the Missouri and pre-evaluation 10th-percentile discharge proxies for the Upper and Lower Mississippi. High-water thresholds are pre-evaluation 90th-percentile discharge proxies in all three basins because a usable stage-discharge rating was not obtained. Event-rate entries are low/high/low-or-high.

Basin	Low trigger (cfs)	Low definition	High trigger (cfs)	High definition	Observed low/high/two-sided
Lower Mississippi	201,096	pre-eval p10 proxy	804,435	pre-eval p90 proxy	0.057 / 0.181 / 0.238
Missouri	47,000	WAP Action cfs	134,142	pre-eval p90 proxy	0.179 / 0.201 / 0.381
Upper Mississippi	37,320	pre-eval p10 proxy	199,279	pre-eval p90 proxy	0.030 / 0.212 / 0.242

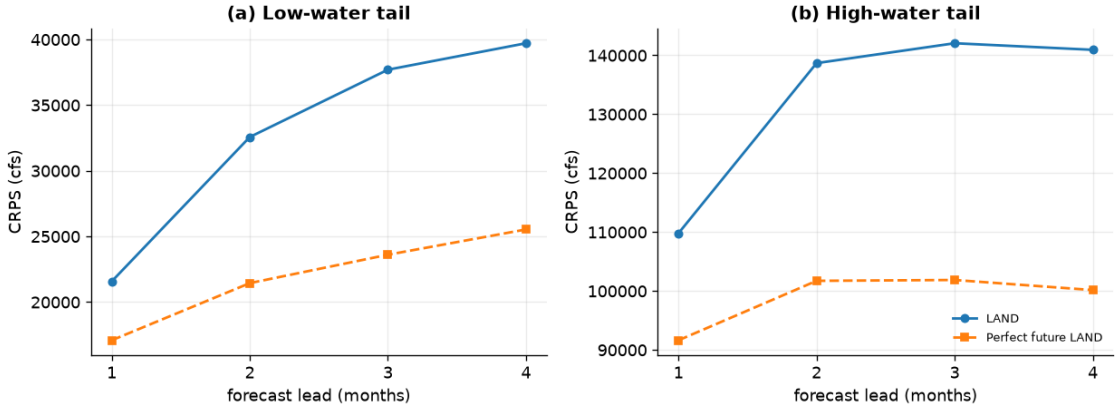


Fig 5. Low-water and high-water tails CRPS across leads 1-4 for operational LAND and perfect-future LAND. Lower CRPS indicates better probabilistic forecasts. Perfect-future LAND substantially reduces forecast error in both tails, with the gap between them increasing with lead.

4.5. Basis risk across the operational horizon

To convert forecast probabilities into payout decisions, a single forecast-probability cutoff (τ) is used for each risk type across all three basins and leads 1-4. For each risk type, τ is selected by testing values from 0.05 to 0.80 in increments of 0.05 and choosing the value that minimizes the mean basis-risk score across the three basins and leads 1-4. The selected cutoffs are τ=0.05 for low water, τ=0.15 for high water, and τ=0.30 for combined low- or high-risk. A payout is triggered when the forecast probability exceeds the relevant cutoff. Basis risk is measured as the average of the missed-disruption rate, when an event occurs but no payout is triggered, and the unnecessary-payout rate, when a payout is triggered but no event occurs. Averaged across the three basins and leads 1-4, the operational LAND basis-risk scores are 0.206 for low water, 0.232 for high water, and 0.304 for combined low-or-high risk. Applying the same probability cutoffs to perfect-future LAND reduces these scores to 0.142, 0.155, and 0.228, respectively (Table 4; Fig 6).

Table 4. Reference decision thresholds and mean basis-risk scores across the three basins and leads 1-4. The basis-risk score is the equal-weight mean of the uncompensated-disruption rate and unnecessary-payout rate. Perfect-future LAND uses the same operating thresholds as operational LAND.

Tail	Reference tau	Operational mean score	Perfect-future mean score	Reduction	Scope
Low water	0.05	0.206	0.142	0.064	3 basins, leads 1-4
High water	0.15	0.232	0.155	0.077	3 basins, leads 1-4
Low or high	0.30	0.304	0.228	0.076	3 basins, leads 1-4

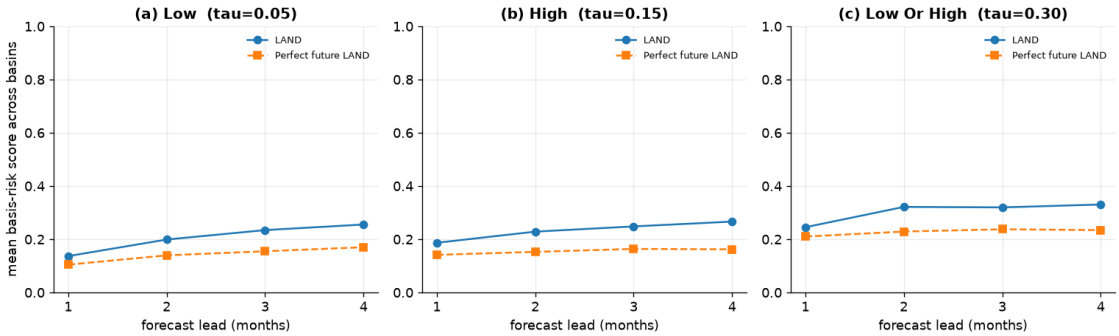


Fig 6. Mean basis-risk score across basins at leads 1-4 for low-water, high-water, and combined low-or-high risk. The score is the equal-weight mean of the missed-disruption rate and unnecessary-payout rate at the risk-specific probability cutoffs shown in Table 4. Solid lines show operational LAND and dashed lines show the perfect-future LAND diagnostic. High-water and combined results are subject to the empirical high-flow proxy limitation.

Basis risk also increases with forecast lead: the mean operational score rises from about 0.136 at lead 1 to 0.255 at lead 4, compared with 0.104 to 0.170 for perfect-future LAND. This indicates that uncertainty in future land conditions contributes to payout errors as forecast lead increases. Basin-, lead-, and risk-specific values are given in S3 Table.

4.6. Nonstationarity of the discharge record

The annual-minimum series used for low-water return-period pricing is stationary over the common 1979-2024 period under the tests used here. Mann-Kendall p values are 0.806 for the Lower Mississippi, 0.712 for the Missouri, and 0.992 for the Upper Mississippi; Pettitt p values are 0.977, 0.461, and 1.000, respectively (S3 Fig). The much longer records do not support a single stationary distribution: all three show significant increasing trends and change points, with Pettitt change years of 1968 for the Lower Mississippi, 1967 for the Missouri, and 1979 for the Upper Mississippi. Accordingly, primary low-water pricing uses the common 1979-2024 period

and the full records are kept only as sensitivity analyses. These stationarity tests apply to annual minima and do not establish stationarity of the proxy high-water tail.

5. Discussion

The main result is that LAND forecasts are most useful at 1-4 month leads. Skill is strongest at one month and remains useful through four months in all three basins, but becomes small at longer leads. Although mean CRPS skill stays slightly positive through month 11, longer forecasts are much less useful. Adding atmospheric and ocean predictors does not restore the lost skill at longer leads. The forecasts still contain useful predictive information, but their uncertainty is not fully calibrated, especially in the Lower Mississippi, where the 10-90% interval contains the observed flow less often than expected. This limitation could be reduced through post-processing or calibration of the predictive distribution to improve interval coverage.

The perfect-future LAND experiment gives a clear target for improvement. Its skill declines only gradually, from 0.441 at lead 1 to 0.344 at lead 4 and 0.293 at lead 12, while operational skill falls much more rapidly. Because this experiment supplies the future land state rather than future discharge, the gap points to the need to project future hydroclimate rather than to add more encoders. The navigation-risk and insurance results show the practical importance of that gap. Mean low- and high-water event probabilities are relatively stable across leads, but basis risk increases because identifying the correct months becomes harder. Perfect-future LAND lowers basis risk for all three tail definitions, showing that better future land-state information would improve the timing of payouts as well as the probabilistic forecast score. It also raises the fair premium for every empirically supported 10- and 20-year low-water product across the three basins and leads 1-4. Those premium differences range from 0.0051 to 0.0140 per $1 maximum payout, so the future-land-state gap is large enough to affect contract price. The 10- and 20-year

products are the most defensible pricing application because their triggers are supported by the primary annual-minimum record and its stationarity tests. The 50-year low-water values are extrapolative and are treated only as sensitivity results. High-water and combined results are useful demonstrations of the two-sided framework, but all high-water thresholds are empirical discharge proxies in this analysis and therefore should not be presented as stage-based operational contracts.

A natural next step is to forecast those future land states. The North American Multi-Model Ensemble (NMME) standard hindcast archive provides monthly precipitation, 2-m temperature, and sea surface temperature [33–35]. The current NMMEv3 operational system adds maximum and minimum 2-m temperature and 200-hPa geopotential height to those core fields [36]. The 2014 Phase II data plan included monthly soil moisture and runoff, along with daily research fields such as snow water equivalent [37]. Those land-state variables are not part of the current NMMEv3 operational set. An extension could combine the available NMME meteorological forecasts with the additional daily forcing, such as wind, needed to run a calibrated land-surface or hydrologic model and generate soil moisture, snow, runoff, and related basin states for Chronos-2. Mo and Lettenmaier [38] demonstrated one version of this approach over the U.S. by bias-correcting and downscaling monthly NMME precipitation and temperature forecasts, constructing daily VIC forcing with sampled historical weather, and producing soil-moisture, snow-water-equivalent, and runoff forecasts out to three months. Yuan et al. [39] extended this approach globally by using NMME forecasts to drive VIC and a river routing model. The resulting six month hindcasts of soil moisture and streamflow outperformed ensemble streamflow prediction for several months, with some drought forecasts retaining skill out to six months. An operational system was developed by Arsenault et al. [40] for Africa, where bias-

corrected and downscaled NASA GEOS (a member of NMME) seasonal forecasts were used with satellite-informed initial conditions in NASA's Land Information System with 1 to 5 month hindcasts capturing major historical drought events. Baker et al. [41] translated CFSv2 and NMME precipitation and temperature forecasts to U.S. watersheds specifically for hydrologic and water-management applications. Other initialized seasonal prediction systems could also be explored as sources of forecast land-surface and atmospheric covariates for this framework. This extension would provide a direct test of how much of the perfect-future LAND gap can be closed.

Forecast skill alone does not establish decision value. Work on flood-risk management has shown the importance of understanding how scientific information and its uncertainty enter actual decisions [42]. For navigation, a further step is to work with shippers and port operators to test whether the forecast probabilities and premium signals fit their planning horizons and change shipment or coverage choices.

6. Conclusions

We developed a framework that links monthly streamflow forecasts to navigation risk, low-water insurance pricing, and basis-risk evaluation for the Mississippi River system. The LAND forecast performs best at 1-4 month leads, with mean CRPS skill of 0.301, 0.153, 0.101, and 0.078. Skill remains slightly above climatology through lead 11 but is small after month 4. The framework evaluates low-water, high-water, and combined risk using separate thresholds and basis-risk measures. The 10- and 20-year low-water products are supported by the 1979-2024 record. Using perfect-future LAND conditions increases fair premiums by 0.0051-0.0140 per $1 of maximum payout. The 50-year low-water trigger is treated as a sensitivity test, while high-water results remain proxy-based.

The perfect-future LAND diagnostic identifies the main opportunity for improvement. Its mean CRPS skill remains 0.344 at four months and 0.293 at twelve months, and it reduces mean basis-risk scores across the 1-4 month horizon from 0.206 to 0.142 for low water, from 0.232 to 0.155 for high water, and from 0.304 to 0.228 for combined risk. NMME forecast protocols extend through at least nine months and can provide initialized precipitation and temperature forcing, but NMME does not provide a complete and uniformly available replacement for the LAND variables. The most direct future work is to downscale seasonal climate forecasts, drive a calibrated land-surface or hydrologic model to predict soil moisture, snow, runoff, and related basin states, and then test whether those forecast land conditions close the gap toward the perfect-future LAND benchmark. Or other initialized seasonal prediction systems could also be used as sources of forecast land-surface and atmospheric covariates.

Forecast-based premiums could help shippers act before navigation is disrupted. For the same coverage, a higher premium would signal greater expected risk, which could lead shippers to delay a shipment or consider rail or truck transport. Forecast skill at 1-4 months could give them time to adjust their plans. Whether that signal changes decisions or reduces losses remains to be tested.

Competing interests: The authors declare no conflicts of interest.

Author Contributions: Conceptualization, J.N., X.N. and U.L.; investigation, J.N.; data curation, J.N.; formal analysis, X.N.; visualization, X.N.; writing (original draft preparation), J.N.; writing (review and editing), J.N., X.N. and U.L. All authors have read and agreed to the published version of the manuscript.

Data Availability Statement: This study analyzed existing observational and reanalysis datasets and generated derived predictors and probabilistic forecasts. The existing data sources are ERA5

monthly surface and pressure-level fields [29] from the Copernicus Climate Data Store (single levels: https://doi.org/10.24381/cds.f17050d7; pressure levels: https://doi.org/10.24381/cds.6860a573); Hadley Centre Sea Ice and Sea Surface Temperature (HadISST) data [31] from the Met Office (https://www.metoffice.gov.uk/hadobs/hadisst/); and Ocean Reanalysis System 5 (ORAS5) upper-ocean heat-content data [32], available through the Copernicus Climate Data Store (https://doi.org/10.24381/cds.67e8eeb7). Discharge and gage-height records are available from the USGS National Water Information System (https://waterdata.usgs.gov/nwis; stations 05587450 and 06934500) and USACE RiverGages (https://rivergages.mvr.usace.army.mil/; Tarbert Landing 01100Q and Red River Landing 01120). Waterways Action Plan navigation thresholds were obtained from the published annexes [4–9].

The derived vertically integrated ERA5 moisture-budget fields used in the LAND predictors are available through http://magog.ldeo.columbia.edu:8080/opendap/hyrax/local/data1/jennie/Tulane/Monthly/OBS/Global/MB/MB194001-202412.nc.dmr.html. The file contains total moisture-flux divergence (Dviqu), monthly-mean-flow moisture-flux divergence (DVIqmum), the related mean-flow divergence term used for the decomposition (VIDqmum), the wind-convergence component (VIqmDum), and the horizontal moisture-advection component (VIumGqm). The analysis uses the 1959-2024 period and area-averages each field over the study basins.

Numerical results are provided in the main and supplementary tables. The analysis and forecasting notebooks are described under Code Availability.

Code Availability: The analysis and forecasting Python notebooks are deposited in an unpublished Zenodo draft (reserved DOI: https://doi.org/10.5281/zenodo.23286424). The DOI

will become active when the record is published. A private preview link will be supplied to the editors and reviewers through the journal submission system; the record will be made publicly available no later than publication of the journal article.

Funding: This work was supported by a Research Stabilization Fund (RSF) award from Columbia University (UR015156) and by an award from the ByWater Institute for Climate Adaptation at Tulane University.

Acknowledgments: The authors thank the sources of the Waterways Action Plan annexes and the operators of the USGS, USACE, and Copernicus data services, as well as Haibo Liu for calculating and providing the ERA5 vertically integrated moisture-budget terms used in this study. J.N. thanks the participants of the Tulane Headwaters to Delta (HW2D) Working Group of the Mississippi Basin Centennial Initiative for discussions that helped inform the broader Mississippi River research context for this work, and Emily Federer of the Port of New Orleans for helpful discussions about Mississippi River navigation and port operations.

References

1. Wetzstein B, Florax R, Foster K, Binkley J. Transportation costs: Mississippi River barge rates. J Commod Mark. 2021;21: 100123.

2. Waterways Council Inc. Low Water Levels Drive Up Grain Transportation Costs. 2023 [cited 2026 Sep 5]. Available from: https://waterwayscouncil.org/media/in-the-news/article/2023/09/low-water-levels-drive-up-grain-transportation-costs

3. Chen Z, Cheng J. Economic consequences of inland waterway disruptions in the Upper Mississippi River region in a changing climate. Ann Reg Sci. 2024;73: 757-794.

4. U.S. Army Corps of Engineers, Little Rock and Tulsa Districts, U.S. Coast Guard, Sector Lower Mississippi River. McClellan-Kerr Arkansas River Navigation System (MKARNS) Waterway Action Plan; U.S. Army Corps of Engineers. 2023 [cited 2026 Jan 10]. Available from: https://www.swl.usace.army.mil/Portals/50/docs/navigation/Assets/Documents/MKARNS%20Waterway%20Action%20Plan%202023-PublicWeb.pdf

5. U.S. Coast Guard, Sector Lower Mississippi River. Mississippi River and Tributaries Waterways Action Plan: Sector Lower Mississippi River Annex; U.S. Department of Homeland Security, Eighth Coast Guard District. 2020 [cited 2026 Jan 10]. Available from: https://www.atlanticarea.uscg.mil/Portals/7/Eigth%20District/Sector%20Lower%20Mississippi%20River/pdf/2020%20WAP%20Annex%20SLMR%20Final.pdf

6. U.S. Coast Guard, Sector Ohio Valley. Waterways Action Plan: Mississippi River, Ohio River, and Tributaries; U.S. Department of Homeland Security, Eighth Coast Guard District. 2021 [cited 2026 Jan 10]. Available from: https://www.atlanticarea.uscg.mil/Portals/7/Eigth%20District/Waterways/docs/2021%20Sector%20Ohio%20Valley%20WAP.pdf

7. U.S. Coast Guard, Sector Upper Mississippi River. Mississippi River and Tributaries Waterways Action Plan: Illinois Waterway Annex; U.S. Department of Homeland Security, Eighth Coast Guard District. 2017 [cited 2026 Jan 10]. Available from: https://www.atlanticarea.uscg.mil/Portals/7/Eigth%20District/WesternRivers/docs/ILR_WAP_2017_Final.pdf

8. U.S. Coast Guard, Sector Upper Mississippi River. Mississippi River and Tributaries Waterways Action Plan: Missouri River Annex; U.S. Department of Homeland Security, Eighth Coast Guard District. 2017 [cited 2026 Jan 10]. Available from: https://www.atlanticarea.uscg.mil/Portals/7/Eigth%20District/WesternRivers/docs/MOR_WAP_2017_Final.pdf

9. U.S. Coast Guard, Sector Upper Mississippi River. Mississippi River and Tributaries Waterways Action Plan: Upper Mississippi River Annex; U.S. Department of Homeland Security, Eighth Coast Guard District. 2017 [cited 2026 Jan 10]. Available from: https://www.atlanticarea.uscg.mil/Portals/7/Eigth%20District/SectorUMR/UMR%20WAP%202017.pdf

10. Amorim R, Villarini G, Veatch W, White K. Reduced and more fragmented Mississippi River navigability by rising flow. Geophys Res Lett. 2023;50: e2023GL104619. doi: 10.1029/2023GL104619.

11. U.S. Department of Agriculture, Agricultural Marketing Service. Grain Transportation Report, 5 October. 2023 [cited 2026 Sep 7]. Available from: https://doi.org/10.9752/TS056.10-05-2023

12. Dryfoos, D., Schmid, E. Mississippi River Towns Pilot New Insurance Model to Help With Disaster Response. Mississippi Free Press. 2024 [cited 2026 Oct 6]. Available from: https://www.mississippifreepress.org/mississippi-river-towns-pilot-new-insurance-model-to-help-with-disaster-response/

13. Dunsavage, J. Parametric Insurance Gains Traction Across U.S. Insurance Information Institute, 12 February. 2025 [cited 2026 Oct 6]. Available from: https://insuranceindustryblog.iii.org/parametric-insurance-gains-traction-across-u-s/

14. Ten Across. Mississippi River Mayors Coalesce to Address Shared Climate Risks, 15 August. 2025 [cited 2026 Oct 6]. Available from: https://10across.org/mississippi-river-mayors-coalesce-to-address-shared-climate-risks/

15. National Association of Insurance Commissioners (NAIC). Affordability and Availability Playbook Outline. 2025 [cited 2026 Oct 6]. Available from: https://content.naic.org/sites/default/files/inline-files/Affordability%20and%20Availability%20Playbook%20Outline_Posted%20For%2010.14%20Open%20Meeting.docx

16. Thornton, K. Traditional Home Insurance Is Collapsing. Here's What Could Fill the Gap. WIRED, 16 June. 2026 [cited 2026 Oct 6]. Available from: https://www.wired.com/story/ai-assisted-parametric-insurance-climate-change/

17. Swiss Re Corporate Solutions. FLOW Parametric Water-Level Insurance. 2024 [cited 2026 Oct 6]. Available from: https://corporatesolutions.swissre.com/dam/jcr:3b534611-27be-4fc1-b2dd-1e570a9d882a/FLOW-parametric-water-level-insurance.pdf

18. Marsh. Navigating Waterways: Climate Change Implications for the Maritime Sector. Feature: The Mississippi River. 2024 [cited 2025 Oct 7]. Available from: https://www.marsh.com/en/risks/climate-change-sustainability/insights/climate-change-implications-maritime-sector.html

19. Khalil AF, Kwon HH, Lall U, Miranda MJ, Skees J. El Niño-Southern Oscillation-based index insurance for floods: Statistical risk analyses and application to Peru. Water Resour Res. 2007;43: W10416. doi: 10.1029/2006WR005281.

20. Sorour H, Uchino T. Effect of changing temperature on the deterioration of soya beans. Biosyst Eng. 2004;87: 453-462.

21. Wang JH, Lin GF, Chang MJ, Huang IH, Chen YR. Real-time water-level forecasting using dilated causal convolutional neural networks. Water Resour Manag. 2019;33: 3759-3780. doi: 10.1007/s11269-019-02342-4.

22. Duan S, Ullrich P, Shu L. Using convolutional neural networks for streamflow projection in California. Front Water. 2020;2: 28. doi: 10.3389/frwa.2020.00028.

23. Yang H, Zhang Z, Liu X, Jing P. Monthly-scale hydro-climatic forecasting and climate change impact evaluation based on a novel DCNN-Transformer network. Environ Res. 2023;236: 116821. doi: 10.1016/j.envres.2023.116821.

24. Nielsen AH, Iosifidis A, Karstoft H. Forecasting large-scale circulation regimes using deformable convolutional neural networks and global spatiotemporal climate data. Sci Rep. 2022;12: 8395. doi: 10.1038/s41598-022-12167-8.

25. Yu F, Koltun V. Multi-scale context aggregation by dilated convolutions. arXiv:1511.07122 [Preprint]. 2015. Available from: https://arxiv.org/abs/1511.07122. doi: 10.48550/arXiv.1511.07122.

26. Ansari AF, Stella L, Turkmen C, Zhang X, Mercado P, Shen H, et al. Chronos: Learning the language of time series. arXiv:2403.07815 [Preprint]. 2024. Available from: https://arxiv.org/abs/2403.07815. doi: 10.48550/arXiv.2403.07815.

27. Ansari AF, Shchur O, Küken J, Auer A, Han B, Mercado P, et al. Chronos-2: From univariate to universal forecasting. arXiv:2510.15821 [Preprint]. 2025. Available from: https://arxiv.org/abs/2510.15821. doi: 10.48550/arXiv.2510.15821.

28. Rantz, S.E., et al. Measurement and Computation of Streamflow, Volume 2: Computation of Discharge; U.S. Geological Survey Water-Supply Paper 2175; U.S. Geological Survey. 1982 [cited 2026 Sep 7]. Available from: https://pubs.usgs.gov/wsp/wsp2175/wsp2175_vol2.pdf

29. Hersbach H, Bell B, Berrisford P, Hirahara S, Horányi A, Muñoz-Sabater J, et al. The ERA5 global reanalysis. Q J R Meteorol Soc. 2020;146: 1999-2049. doi: 10.1002/qj.3803.

30. Seager R, Henderson N. Diagnostic computation of moisture budgets in the ERA-Interim reanalysis with reference to analysis of CMIP-archived atmospheric model data. J Clim. 2013;26: 7876-7901.

31. Rayner NA, Parker DE, Horton EB, Folland CK, Alexander LV, Rowell DP, et al. Global analyses of sea surface temperature, sea ice, and night marine air temperature since the late nineteenth century. J Geophys Res Atmos. 2003;108(D14): 4407. doi: 10.1029/2002JD002670.

32. Zuo H, Balmaseda MA, Tietsche S, Mogensen K, Mayer M. The ECMWF operational ensemble reanalysis-analysis system for ocean and sea ice: a description of the system and assessment. Ocean Sci. 2019;15: 779-808. doi: 10.5194/os-15-779-2019.

33. Kirtman BP, Min D, Infanti JM, Kinter JL 3rd, Paolino DA, Zhang Q, et al. The North American multimodel ensemble: phase-1 seasonal-to-interannual prediction; phase-2 toward developing intraseasonal prediction. Bull Am Meteorol Soc. 2014;95: 585-601. doi: 10.1175/BAMS-D-12-00050.1.

34. Becker EJ, Kirtman BP, L'Heureux M, Muñoz ÁG, Pegion K. A decade of the North American Multimodel Ensemble (NMME): Research, application, and future directions. Bull Am Meteorol Soc. 2022;103: E973-E995. doi: 10.1175/BAMS-D-20-0327.1.

35. NOAA Climate Prediction Center. NMME User's Guide. NOAA/NWS/NCEP Climate Prediction Center. 2026 [cited 2026 Oct 11]. Available from: https://ftp.cpc.ncep.noaa.gov/NMME/archive/2026040800/users_guide.html

36. NOAA Climate Prediction Center. NMMEv3 Operational User Manual. NOAA/NWS/NCEP Climate Prediction Center. 2026 [cited 2026 Oct 11]. Available from: https://ftp.cpc.ncep.noaa.gov/CPC/ID/figs/USER_MANUAL.html

683 37. NOAA Climate Prediction Center. NMME Phase-II Data Plan. NOAA/NWS/NCEP Climate
684 Prediction Center, 27 May. 2014 [cited 2026 Oct 11]. Available from:
685 https://www.cpc.ncep.noaa.gov/products/CTB/Documents/NMME-PhaseII-DataPlan-
686 27May.pdf

687 38. Mo KC, Lettenmaier DP. Hydrologic prediction over the conterminous United States using
688 the national multi-model ensemble. J Hydrometeorol. 2014;15: 1457-1472.

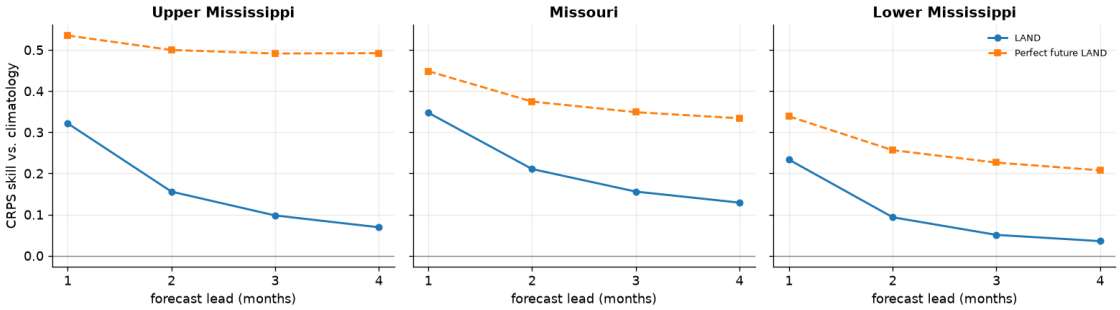
689 39. Yuan X, Roundy JK, Wood EF, Sheffield J. Seasonal forecasting of global hydrologic
690 extremes: System development and evaluation over GEWEX basins. Bull Am Meteorol Soc.
691 2015;96: 1895-1912.

692 40. Arsenault KR, Shukla S, Hazra A, Getirana A, McNally A, Kumar SV, et al. The NASA
693 hydrological forecast system for food and water security applications. Bull Am Meteorol
694 Soc. 2020;101: E1007-E1025. doi: 10.1175/BAMS-D-18-0264.1.

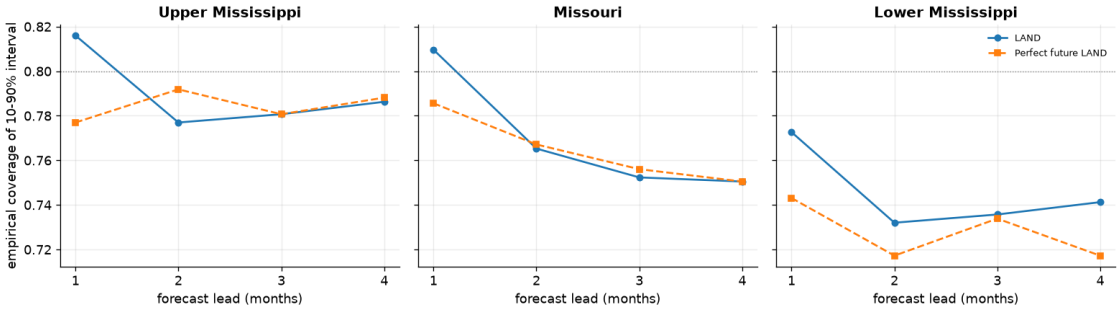
695 41. Baker SA, Wood AW, Rajagopalan B. Developing subseasonal to seasonal climate forecast
696 products for hydrology and water management. J Am Water Resour Assoc. 2019;55: 1024-
697 1037.

698 42. Morss RE, Wilhelmi OV, Downton MW, Gruntfest E. Flood risk, uncertainty, and scientific
699 information for decision making: Lessons from an interdisciplinary project. Bull Am
700 Meteorol Soc. 2005;86: 1593-1602. doi: 10.1175/BAMS-86-11-1593.

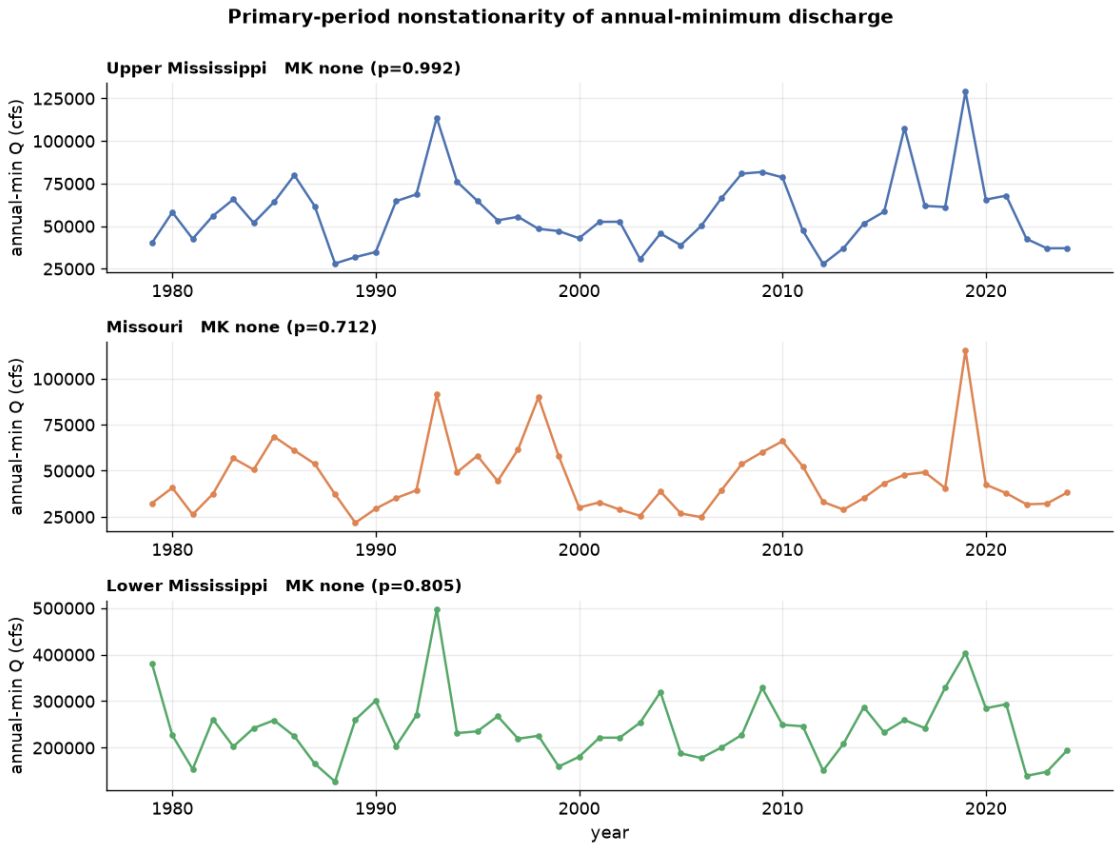
Supporting information



S1 Fig. Basin-level CRPS skill versus climatology for operational LAND and perfect-future LAND across leads 1-4. The diagnostic gap is largest at longer leads and is especially pronounced for the Upper Mississippi.



S2 Fig. Coverage of the 10-90% forecast interval at leads 1-4 for LAND and perfect-future LAND in each basin. The dotted line shows the expected 80% coverage.



S3 Fig. Primary period annual minimum monthly discharge by basin with Mann-Kendall trend-test results. Pettitt tests also find no significant primary period change point. Full-record sensitivity tests are nonstationary in all three basins.

Supporting tables

S1 Table. Fair premiums for the 10- and 20-year low-water products are shown by basin and forecast lead. LAND is the operational forecast, while perfect-future LAND is used only for comparison. The 50-year trigger is included only as a sensitivity test.

Basin	Lead	Return period	Trigger (cfs)	LAND premium	Perfect-future premium	Difference
Upper Mississippi	1	10-yr	35,675	0.0246	0.0367	+0.0121

Basin	Lead	Return period	Trigger (cfs)	LAND premium	Perfect-future premium	Difference
Upper Mississippi	1	20-yr	30,844	0.0146	0.0239	+0.0093
Upper Mississippi	2	10-yr	35,675	0.0258	0.0398	+0.0140
Upper Mississippi	2	20-yr	30,844	0.0158	0.0265	+0.0107
Upper Mississippi	3	10-yr	35,675	0.0290	0.0408	+0.0118
Upper Mississippi	3	20-yr	30,844	0.0185	0.0280	+0.0095
Upper Mississippi	4	10-yr	35,675	0.0303	0.0414	+0.0111
Upper Mississippi	4	20-yr	30,844	0.0196	0.0288	+0.0092
Missouri	1	10-yr	27,840	0.0221	0.0295	+0.0074
Missouri	1	20-yr	25,710	0.0163	0.0229	+0.0066
Missouri	2	10-yr	27,840	0.0219	0.0316	+0.0097
Missouri	2	20-yr	25,710	0.0166	0.0248	+0.0082
Missouri	3	10-yr	27,840	0.0210	0.0318	+0.0108
Missouri	3	20-yr	25,710	0.0159	0.0252	+0.0093
Missouri	4	10-yr	27,840	0.0214	0.0317	+0.0103
Missouri	4	20-yr	25,710	0.0163	0.0252	+0.0088
Lower Mississippi	1	10-yr	156,752	0.0102	0.0165	+0.0063
Lower Mississippi	1	20-yr	148,944	0.0087	0.0138	+0.0051
Lower Mississippi	2	10-yr	156,752	0.0103	0.0183	+0.0080
Lower Mississippi	2	20-yr	148,944	0.0090	0.0154	+0.0065

Basin	Lead	Return period	Trigger (cfs)	LAND premium	Perfect-future premium	Difference
Lower Mississippi	3	10-yr	156,752	0.0111	0.0209	+0.0097
Lower Mississippi	3	20-yr	148,944	0.0096	0.0176	+0.0080
Lower Mississippi	4	10-yr	156,752	0.0120	0.0233	+0.0113
Lower Mississippi	4	20-yr	148,944	0.0100	0.0196	+0.0096

S2 Table. Low-, high-, and combined-water navigation probabilities are shown by basin and forecast lead. Observed event rates use the same verification months at each lead. High-water probabilities are based on empirical high-flow discharge thresholds.

Basin	Lead	Tail	LAND probability	Perfect-future probability	Observed rate
Lower Mississippi	1	Low water	0.038	0.048	0.057
Lower Mississippi	1	High water	0.165	0.160	0.181
Lower Mississippi	1	Low or high	0.202	0.208	0.238
Lower Mississippi	2	Low water	0.035	0.051	0.057
Lower Mississippi	2	High water	0.162	0.158	0.181
Lower Mississippi	2	Low or high	0.197	0.209	0.238
Lower Mississippi	3	Low water	0.039	0.055	0.057
Lower Mississippi	3	High water	0.165	0.159	0.181
Lower Mississippi	3	Low or high	0.204	0.215	0.238

Basin	Lead	Tail	LAND probability	Perfect-future probability	Observed rate
Lower Mississippi	4	Low water	0.043	0.060	0.057
Lower Mississippi	4	High water	0.171	0.165	0.181
Lower Mississippi	4	Low or high	0.215	0.225	0.238
Missouri	1	Low water	0.180	0.181	0.179
Missouri	1	High water	0.186	0.177	0.201
Missouri	1	Low or high	0.366	0.359	0.381
Missouri	2	Low water	0.176	0.184	0.179
Missouri	2	High water	0.182	0.167	0.201
Missouri	2	Low or high	0.357	0.351	0.381
Missouri	3	Low water	0.172	0.180	0.179
Missouri	3	High water	0.182	0.168	0.201
Missouri	3	Low or high	0.355	0.349	0.381
Missouri	4	Low water	0.173	0.175	0.179
Missouri	4	High water	0.185	0.180	0.201
Missouri	4	Low or high	0.357	0.355	0.381
Upper Mississippi	1	Low water	0.029	0.042	0.030
Upper Mississippi	1	High water	0.175	0.174	0.212
Upper Mississippi	1	Low or high	0.204	0.216	0.242
Upper Mississippi	2	Low water	0.030	0.045	0.030
Upper Mississippi	2	High water	0.170	0.165	0.212

Basin	Lead	Tail	LAND probability	Perfect-future probability	Observed rate
Upper Mississippi	2	Low or high	0.200	0.210	0.242
Upper Mississippi	3	Low water	0.034	0.046	0.030
Upper Mississippi	3	High water	0.173	0.168	0.212
Upper Mississippi	3	Low or high	0.207	0.214	0.242
Upper Mississippi	4	Low water	0.035	0.047	0.030
Upper Mississippi	4	High water	0.175	0.172	0.212
Upper Mississippi	4	Low or high	0.210	0.219	0.242

S3 Table. Detailed basis risk scores by basin, lead, and navigation tail. The score is the equal weight mean of the uncompensated-disruption rate and unnecessary-payout rate. The same tail specific operating threshold is used for operational LAND and perfect-future LAND.

Basin	Lead	Tail	Tau	LAND basis risk	Perfect-future basis risk	Reduction
Lower Mississippi	1	Low water	0.05	0.094	0.074	+0.020
Missouri	1	Low water	0.05	0.188	0.185	+0.003
Upper Mississippi	1	Low water	0.05	0.127	0.054	+0.073
Lower Mississippi	2	Low water	0.05	0.196	0.141	+0.055
Missouri	2	Low water	0.05	0.232	0.210	+0.022
Upper Mississippi	2	Low water	0.05	0.168	0.067	+0.101

Basin	Lead	Tail	Tau	LAND basis risk	Perfect-future basis risk	Reduction
Lower Mississippi	3	Low water	0.05	0.224	0.170	+0.054
Missouri	3	Low water	0.05	0.256	0.221	+0.035
Upper Mississippi	3	Low water	0.05	0.222	0.073	+0.149
Lower Mississippi	4	Low water	0.05	0.200	0.163	+0.037
Missouri	4	Low water	0.05	0.298	0.246	+0.052
Upper Mississippi	4	Low water	0.05	0.267	0.101	+0.166
Lower Mississippi	1	High water	0.15	0.199	0.169	+0.030
Missouri	1	High water	0.15	0.196	0.164	+0.032
Upper Mississippi	1	High water	0.15	0.164	0.091	+0.073
Lower Mississippi	2	High water	0.15	0.233	0.204	+0.029
Missouri	2	High water	0.15	0.234	0.167	+0.067
Upper Mississippi	2	High water	0.15	0.218	0.086	+0.132
Lower Mississippi	3	High water	0.15	0.274	0.214	+0.060
Missouri	3	High water	0.15	0.245	0.175	+0.070
Upper Mississippi	3	High water	0.15	0.226	0.101	+0.125
Lower Mississippi	4	High water	0.15	0.288	0.197	+0.091
Missouri	4	High water	0.15	0.274	0.196	+0.078
Upper Mississippi	4	High water	0.15	0.236	0.092	+0.144

Basin	Lead	Tail	Tau	LAND basis risk	Perfect-future basis risk	Reduction
Lower Mississippi	1	Low or high	0.30	0.277	0.240	+0.037
Missouri	1	Low or high	0.30	0.271	0.252	+0.019
Upper Mississippi	1	Low or high	0.30	0.187	0.138	+0.049
Lower Mississippi	2	Low or high	0.30	0.345	0.267	+0.078
Missouri	2	Low or high	0.30	0.334	0.277	+0.057
Upper Mississippi	2	Low or high	0.30	0.285	0.142	+0.143
Lower Mississippi	3	Low or high	0.30	0.315	0.282	+0.033
Missouri	3	Low or high	0.30	0.337	0.278	+0.059
Upper Mississippi	3	Low or high	0.30	0.307	0.152	+0.155
Lower Mississippi	4	Low or high	0.30	0.339	0.301	+0.038
Missouri	4	Low or high	0.30	0.353	0.266	+0.087
Upper Mississippi	4	Low or high	0.30	0.299	0.135	+0.164

723